

DDC FILE COPY AD A058709

AFAL-TR-77-193

LEVEL

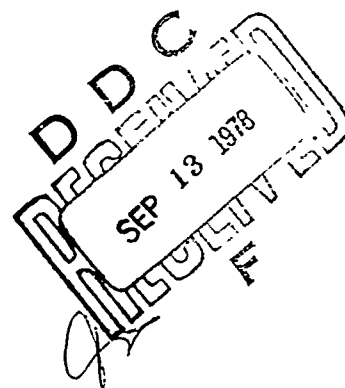
2



ON THE DEVELOPMENT OF SPACE OBJECT OPTICAL AND LWIR  
CROSS SECTION POPULATION DISTRIBUTIONS FROM UHF  
CROSS SECTIONS

Reconnaissance and Weapon Delivery Division

December 1977  
TECHNICAL REPORT AFAL-TR-77-193  
Final Report for Period July 1972 - June 1974



Approved for public release; distribution unlimited

OPOS OBSERVATORY  
AIR FORCE AVIONICS LABORATORY  
Air Force Wright Aeronautical Laboratory, AFSC  
Wright-Patterson Air Force Base, Ohio 45433

78 09 12 007

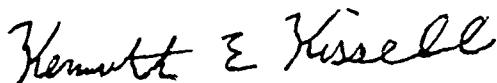
NOTICE

When Government drawings, specifications, or other data are used for any purpose other than in connection with a definitely related Government procurement operation, the United States Government thereby incurs no responsibility nor any obligation whatsoever; and the fact that the government may have formulated, furnished, or in any way supplied the said drawings, specifications, or other data, is not to be regarded by implication or otherwise as in any manner licensing the holder or any other person or corporation, or conveying any rights or permission to manufacture, use, or sell any patented invention that may in any way be related thereto.

This report has been reviewed by the Information Office (OI) and is releasable to the National Technical Information Service (NTIS). At NTIS, it will be available to the general public, including foreign nations.

This technical report has been reviewed and is approved for publication.

FOR THE COMMANDER



DR. KENNETH E. KISSELL, Senior Scientist  
Reconnaissance and Weapon Delivery Division

APPROVED BY:



ROBERT E. DEAL, Acting Asst Chief  
Reconnaissance and Weapon Delivery Division

*"If your address has changed, if you wish to be removed from our mailing list, or if the addressee is no longer employed by your organization please notify AFAL/RW, W-PAFB, OH 45433 to help us maintain a current mailing list".*

*Copies of this report should not be returned unless return is required by security considerations, contractual obligations, or notice on a specific document.*

REPORT DOCUMENTATION PAGE		READ INSTRUCTIONS BEFORE COMPLETING FORM	
1. REPORT NUMBER AFAL-TR-77-193	2. GOVT ACCESSION NO.	3. RECIPIENT'S CATALOG NUMBER	
4. TITLE (and Subtitle) On the Development of Space Object Optical and LWIR Cross Section Population Distributions from UHF Cross Sections.		5. TYPE OF REPORT & PERIOD COVERED Final Technical Report, July 1972-June 1974.	
7. AUTHOR(s) Kenneth E. Kissell, Eugene Muschell, Richard C. Vanderburg		8. CONTRACT OR GRANT NUMBER(s)	
9. PERFORMING ORGANIZATION NAME AND ADDRESS Surveillance Branch (RW) AF Avionics Laboratory Wright-Patterson AFB, Ohio 45433		10. PROGRAM ELEMENT, PROJECT, TASK AREA & WORK UNIT NUMBERS 62204 F 7668-03-17	
11. CONTROLLING OFFICE NAME AND ADDRESS Reconnaissance and Weapon Delivery Division (RW) AF Avionics Laboratory Wright-Patterson AFB, Ohio 45433		12. REPORT DATE December 1977	
14. MONITORING AGENCY NAME & ADDRESS (if different from Controlling Office)		13. NUMBER OF PAGES 22	
16. DISTRIBUTION STATEMENT (of this Report)  Approved for public release; distribution unlimited		15. SECURITY CLASS. (of this report)  Unclassified	
17. DISTRIBUTION STATEMENT (of the abstract entered in Block 20, if different from Report)		15a. DECLASSIFICATION/DOWNGRADING SCHEDULE	
18. SUPPLEMENTARY NOTES			
19. KEY WORDS (Continue on reverse side if necessary and identify by block number) Optical Signatures Detectability of Space Objects Optical Cross Sections LWIR Cross Sections Radar Cross Sections			
20. ABSTRACT (Continue on reverse side if necessary and identify by block number)  See Reverse			

011 670

LB

UNCLASSIFIED

SECURITY CLASSIFICATION OF THIS PAGE (When Data Entered)



The resident population of artificial satellites is everchanging, with new spacecraft and debris being orbited almost daily and older space objects decaying or commanded to earth. Decisions about deployment of future surveillance systems, in most cases requiring 5-10 years of development work before being placed in operation, must be based on a projection of the workload and target detectability which will exist in the future. This report extends to optical detection a rationale used by ADCOM to develop a future radar population. Using this radar population and empirical relationships between optical and UHF radar cross sections in the 1973 satellite population, it predicts the mean optical scattering of sunlight to be 45% of the UHF radar scattering. An analytical model is used to approximate the long-wavelength infrared (LWIR) target brightness in more-complex analogy to radar cross section. This results in a prediction that the mean LWIR cross section will be some 55% greater than the UHF radar cross section but with an uncertainty of a factor 4 in the cross section, i.e., the mean LWIR cross section should lie between 0.4X to 6.2X the UHF cross section depending on the surface materials of the spacecraft.



UNCLASSIFIED

SECURITY CLASSIFICATION OF THIS PAGE (When Data Entered)

FOREWORD

The report develops estimates of the optical brightness of near-earth satellites in the visible and long-wavelength infrared (LWIR) utilizing the extensive data base obtained in the basic research programs under Project 7114, Work Unit 00-03, "Remote Sensing of Space Objects at Optical Wavelengths", at the Aerospace Research Laboratories from 1962 to 1972, and Work Unit 7660-03-17, "Space Object Optical Signatures", funded under Program Element 62204F at the Air Force Avionics Laboratory and carried out by the Surveillance Branch, Reconnaissance and Weapon Delivery Division from 1972 to 1975. Both the ARL and AFAL programs were carried out under a general acronym OPOS, the Optical Properties of Orbiting Spacecraft which also concerned itself with the dynamics, detectability and survivability of space objects.

ACCESSION for	
NTIS	W. H. S. 171 <input checked="" type="checkbox"/>
DDC	B. H. S. 171 <input type="checkbox"/>
UNANNOUNCED	<input type="checkbox"/>
JUSTIFICATION	<input type="checkbox"/>
BY	
DISTRIBUTION AUTHORITY CODES	
A	

TABLE OF CONTENTS

	<u>Page</u>
Introduction	1
Optical Cross Sections	1
Example of Optical Cross Section	2
Source of Optical Cross Section Data	3
Data Base of This Study	3
Presentation of the Data Base	5
Relationship of Optical and Radar Cross Section	5
Maximum Optical Cross Section	8
Consideration of LWIR Cross Section	8
Recommendations	12
Appendix	13
References	20

LIST OF ILLUSTRATIONS

FIGURE		PAGE
1	Optical Cross Section Distribution of 20 Distinct Space Objects	6
2	Distribution of Optical Cross Section of 120 Space Objects in the 30 June 1973 Propulsion	7
3	Comparison of Mean Optical and Radar Cross Sections of 18 Spacecraft for which UHF Data are Available	9
4	Derived Cross Section Populations in Optical, LWIR, and UHF Regions	10
5	Comparison of Maximum Optical and Radar Cross Sections of 18 Spacecraft for which UHF Data are Available	11

## INTRODUCTION

The AFAL program in Deep Space Surveillance under Project 7660 included three major phases related to the SPACETRACK Augmentation Program. These are (1) the evaluation of imaging sensors in the visible light region of the spectrum, (2) the measurement of optical signatures (variations of brightness as a function of time and geometry) of spacecraft for SOI purposes, and (3) the measurement of LWIR signatures of spacecraft for SOI purposes. The latter remained in the hardware implementation stage in two separate approaches, and there is as yet no data base. The imaging sensor evaluation was coupled into the SPACETRACK Augmentation Tradeoff Study (SATS) through the system options studies. This SATS study was conducted by the AFSC Office for the Assistant for Support Studies (OAS) at Kirtland AFB. This memorandum concerns the forecast of future population for resident space objects (RSO). An attempt is also made to relate the existing optical cross-section data base to a probable LWIR cross section data base. As will be brought out, an LWIR data base is an urgently needed item. Possibilities for acquiring this LWIR data base will be discussed in the recommendations.

## OPTICAL CROSS SECTIONS

Recent interest<sup>1</sup> in the concept of the "optical cross section" of orbiting space objects has lead us to look for the existence of established standards, comparable to those which exist<sup>2</sup> for "radar cross section". An attempt will be made in this report to establish optical cross section data for a few space objects patterned as closely as practicable to corresponding radar standards. The very much shorter wavelengths, and the effects of quasi-Lambertian scattering from diffuse surfaces make some departures from the familiar radar models inevitable.

For the measurement of the intensity of sunlight scattered by orbiting objects to an airborne or ground-based sensor to serve as a standard indicator of optical cross section, some or all of the following parameters affect the results: object shape and surface characteristics, spatial orientation (if object shape is non-spherical), albedo or reflectivity of the object, illumination and observational geometries, and the correction of the received light for effects of atmospheric extinction, slant range, and photometer response. If the measurements are performed in other than a single pure color (as were those in the AFAL OPOS program where a broad spectral band was centered in the visual region), there would be additional accountable second-order effects upon the results if different detectors are used. In this report all sensing is broad-band via a photomultiplier with an S-20 photocathode, but will be considered as an equivalent to a single near color in the green region of the spectrum. Because of its independence from illumination, observation and orientation geometries, a perfectly-reflecting specular sphere is chosen as the optical cross-section standard for shape and surface, just as an isotropically-scattering, perfectly-conductive sphere is used as the radar standard.

For diffuse spheres, specular and diffuse cylinders, and flat plates where the scattering follows a Lambertian or other analytical scattering law, one can develop expressions which relate dimensions of the actual body to the apparent brightness. Here we will take the lead of the radar technologists and simply define the optical cross-section as the projected area of a perfectly reflective specular sphere which would yield the same apparent brightness of the target if the sphere and the target were both observed at a distance of 1000 km. In actual fact the sphere and the target would both have the same apparent brightness at any distance if the observing geometry (phase angle, etc.) were the same, but the standardization at 1000 km will allow a second scale to be applied to the data presentation, a scale which gives apparent visual stellar magnitude for the target by a simple adjustment for inverse square law to the data presented.

EXAMPLE OF OPTICAL CROSS SECTION:

It has been shown (Zirker, Whipple and Davis<sup>3</sup>) that the brightness of a perfectly specular sphere is independent of the illumination (or phase) angle:

$$(1) E_o = \frac{E_s b^2}{4R^2} = \frac{E_s (\pi b^2)}{4\pi R^2} \text{ where}$$

$E_o$  = observed flux (with atmospheric extinction removed)  
 $E_s$  = solar flux  
 $b$  = radius of sphere  
 $R$  = slant range

The projected area of the sphere is  $\pi b^2 = \sigma_{opt}$ , the optical cross section.

As an example, it has also been shown<sup>3</sup> that the brightness of a perfectly-diffuse, 100-percent reflecting sphere is:

$$(2) E_o = \frac{2E_s b^2}{3\pi R^2} [\sin \phi + (\pi - \phi) \cos \phi]$$

or (3)  $\sigma_{opt} = \frac{8b^2}{3} [\sin \phi + (\pi - \phi) \cos \phi]$

If  $\phi$  is chosen to be  $83.710^\circ$ , then equations (1) and (2) apply equally.

Similar expressions can be derived for flat plates, cones, and composite bodies.

#### SOURCE OF OPTICAL CROSS SECTION DATA:

The basic source of data on optical cross sections are photoelectric measurements made at the AFAL Optical Properties of Spacecraft (OPOS) observatory, until 1975 located at the John Bryan State Park (JBSP) facility of the AF Avionics Laboratory. Since 1962 measurements have been made of the brightness and brightness variations of spacecraft orbiting over the North American Continent. Raw data exist on some 350 space objects on more than 2000 transits. A small fraction of these signatures or light curves have been fully reduced to standard values of slant range, phase angle, etc. with appropriate corrections for atmospheric absorption. This report takes data which had been reduced on some three dozen objects and presents it in a form to allow projections on the statistical distribution of the brightness to be encountered in the total space population, particularly in the population to be expected in 1980. The extrapolation problem to 1980 is treated in a similar way to the approach for radar population of Ref. 2.

#### DATA BASE OF THIS STUDY:

The apparent optical brightness of 36 spacecraft of 20 known different types were available as the basic data. Light curves of these spacecraft, which include both payloads and rocket bodies, are representative of at least 115 objects typically in orbit on 30 June 1973, when approximately 570 payloads and perhaps 250 rocket bodies were in orbit out to synchronous altitude. Some of the specific objects used were no longer in earth orbit, having decayed since the measurements were made. Sixteen (16) of the twenty vehicle types and 28 of the 36 vehicles remained in orbit at the epoch date (30 June 1973). The brightness data were already adjusted to the 1000-km slant range. The light curves were examined for the faintest value (minimum optical cross section), maximum value (maximum cross section) and temporal mean value (mean optical cross section). The specific vehicles are not identified here in order to avoid a classification problem associated with the source of the radar cross-section data. These optical data are presented in Table I where the values given are those observed for the class of object. The table also lists the 30 June 1973 population. The sampled population includes 32 synchronous or quasi-synchronous objects.

The data used here, for the most part, have been published in References 4 to 14, supplemented by unpublished results obtained in early 1974 at the close of the OPOS program. The data reduction techniques are reported in Refs. 4, 13, 15 and 16.

Table I. Optical Cross Sections Determined  
at the AFAL OPOS Observatory

<u>Object Type</u>	<u>Log X-Section</u>			<u>Nr of this object type in orbit on 30 June 1973</u>
	<u>Max</u>	<u>Mean</u>	<u>Min</u>	
1	1.11	.74	.04	2
2	.74	.52	.05	3
3	.52	-.92	-1.22	48
4	1.20	-0.40	-1.10	4
5	.20	.72	.04	4
6	1.68	1.12	.48	0
7	3.94	1.70	1.22	4
8	-.04	-.11	-.20	3
9	.68	.49	.11	1
10	2.44	1.70	1.00	1
11	1.00	.70	-.64	2
12	.88	.65	.16	1
13	3.00	2.86	1.60	1
14	1.60	1.00	-.80	2
15	1.60	1.00	.40	2
16	2.06	1.43	-.54	15
17	.61	.46	.22	13
18	.78	.70	-.64	4
19	-.74	-.77	-.30	4
20	1.30	-0.80	-0.80	5
				<u>120</u> Total

## PRESENTATION OF THE DATA BASE.

The problem of using a few selected objects to characterize the properties of a large population is a thorny statistical one, analogous to predicting an election on a few scattered returns. Figure 1 presents the distribution of optical cross section within the selected object types. If one could assume a population of payloads and rocket bodies which has the same general composition as the objects represented here, the distribution of max, mean and min cross-section could be used as presented. Because our selection of objects for SOI analysis is completely unrelated to an attempt to "represent" the population, this proportionality assumption seems unlikely, but may in fact exist. This totally ignores the 2000 - plus objects classed as fragments or debris. These debris objects are ignored out of ignorance since we never concerned ourselves with objects other than payloads and upper stages in the OPOS program. These fragments also are presumed smaller in size and of peculiar shape in those cases where they result from catastrophic failures. Others will be protective covers, despin cables, etc. which could occasionally give a bright glint but whose mean cross section should be small.

A second attempt to present the data is to show the optical cross-section distribution of the 115 objects in orbit as of 30 June 1973, ignoring all of the other 600 to 700 objects. This distribution is strongly peaked by the large population increment due to the "Object Type 3" payloads of which at least 48 were in orbit and possibly 62. This distribution function is shown in Figure 2 where the Type 3 peaks are obvious. It should be pointed out that other "operational" spacecraft would be represented by similar peaks as would standardized upper stages such as the "Lunik" and "Venik" stages believed to orbit many USSR payloads, and the Burner II and Altair upper stages used for many U.S. vehicles.

## RELATIONSHIP OF OPTICAL AND RADAR CROSS SECTION.

In the course of discussions with the Office for the Assistant for Support Studies (OAS) on 24 August 1973, regarding the difficulty in extrapolating the data base to the complete population or to the future population, it was suggested that it might be of value to look at the optical cross-section data in comparison to the more complete data base on radar cross-section. The only readily-available radar data are those in the UHF region. The SOI Summary (SOISUM) issued monthly by the ADCOM SDC contains two entries on each cataloged object, a mean UHF cross section and a maximum UHF cross section. Discussions held with Mr. Lloyd Anderson of CALSPAN Corp., one of the most experienced of the radar SOI workers in the country, led to the conclusion that if the tabulated mean UHF cross section is a valid average over the  $4\pi$  steradians of the object's surface, it should be expected to be slightly greater than the optical cross section since it will represent the true mean cross section of the target as the result of the surface conductivity being nearly infinite at the UHF frequency. One would also expect that the "mean" radar cross section at other frequencies (L, S, C, etc.) to be essentially the same as the mean UHF cross section. On the other hand, the mean optical cross section should be lower because the optical reflectivity of any surface is somewhat less than 100%. White paints and polished aluminum reflect only 80-95%, and spacecraft surfaces

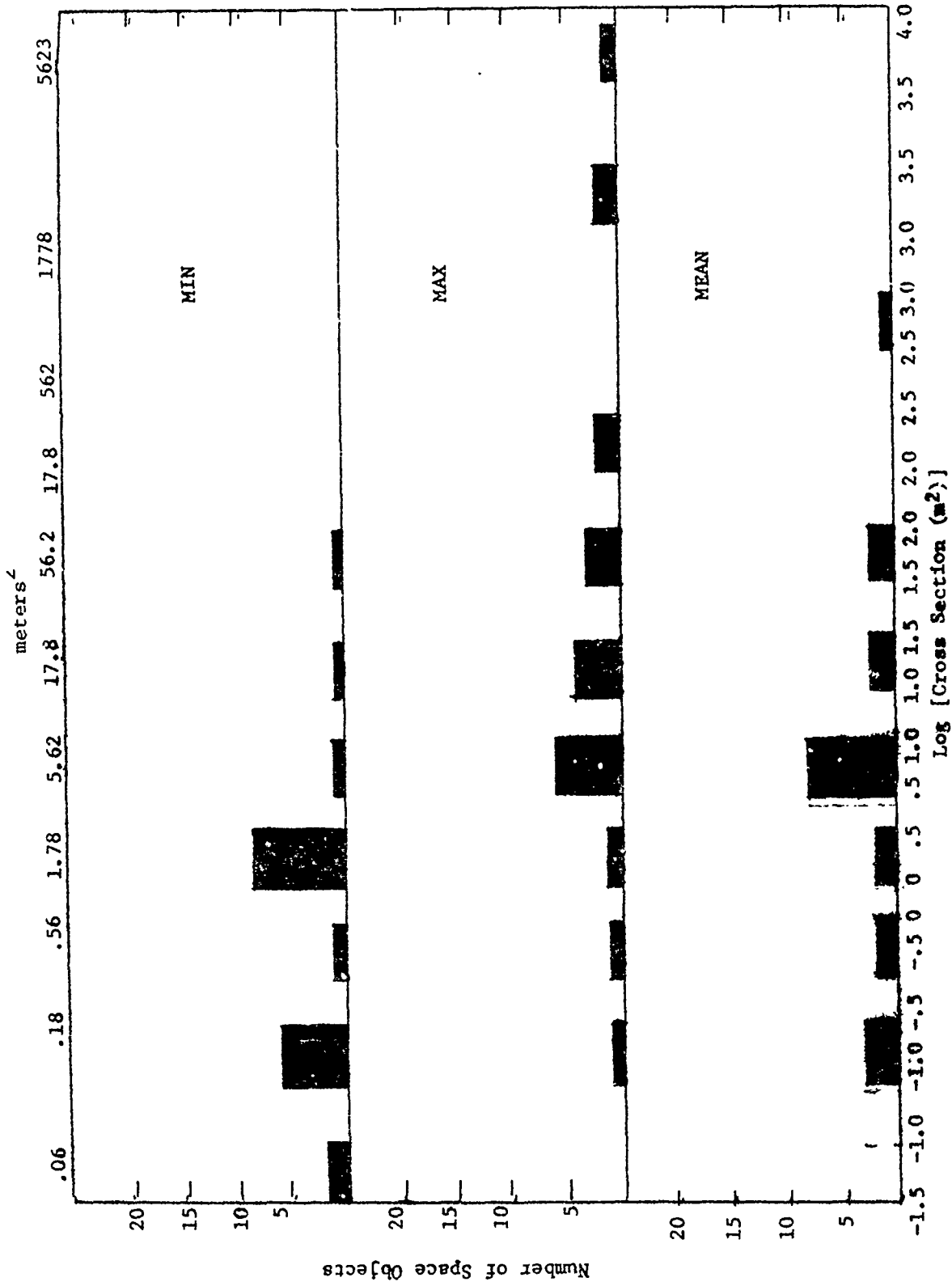


FIGURE 1. OPTICAL CROSS SECTION DISTRIBUTION OF 20 DISTINCT SPACE OBJECTS

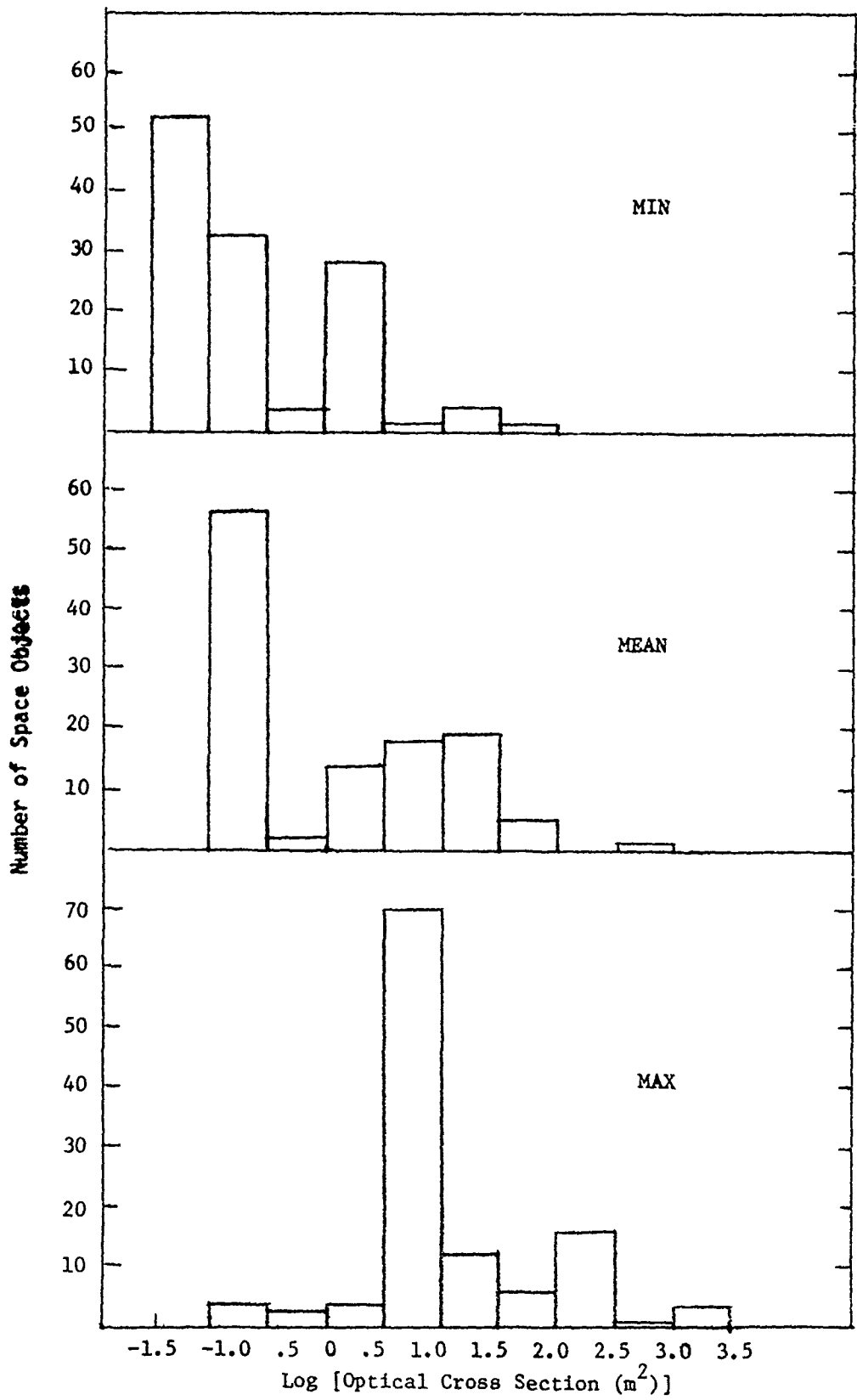


FIG. 2. DISTRIBUTION OF OPTICAL CROSS SECTION OF 120 SPACE OBJECTS IN THE 30 JUNE 1973 PROPULSION

consist only in part of high-reflectivity materials.

Figure 3 shows the comparison of mean UHF radar cross section versus mean optical cross section on the 18 vehicle types for which the SOISUM contained data. The one large mean cross section object is PAGEOS which was designed to have a nearly perfect optical cross section as well as a nearly perfect radar cross section. On the remaining objects, optical cross section lies approximately 0.35 in the log to the left of the 45° diagonal. This translates into a factor of approximately 0.45 between the mean optical cross section and the mean UHF cross section. If this could be validated over a broader data base, any projection of UHF cross-section population could be translated into an optical cross section population by reducing the cross sections by a factor of 0.45X. This is probably the best method to be used in any population study at this time. The scatter in the limited data on hand is less than one order of magnitude, which seems as good as the mean UHF cross-section data according to discussions with Capts Rue and Huner of ADCOM. Figure 4 is a plot of such an optical cross-section distribution function based on the 1971 population of Ref 2. It is obtained by shifting the abscissa of Ref 2, Figure C-2 by 0.34 in log or 0.80 in natural log (which the user should note was used in Ref 2), so as to reduce the cross section.

#### MAXIMUM OPTICAL CROSS SECTION

Discussions were also held with Mr. Anderson of CALSPAN Corp. on the relationship to be expected in maximum radar cross section and maximum optical cross section. Here the radar cross section is known to vary with frequency such that the peak cross section will increase from the VHF through the UHF and up to C-band as the flat and cylindrical speculars sharpen in their directivity. This increase in cross section will not extend to optical frequencies, however, since the surfaces of these elements are not of optical quality in the visible spectrum, except in a handful of unique cases where windows or optical surfaces might be involved. These optical surfaces might not be those responsible for radar returns if they are non-conductive.

It is not possible to estimate, on physical arguments, the degree to which the maximum optical cross section might be less than the maximum radar cross section. The experimental data on 18 objects shows that the max optical cross section seems to be less than even the max UHF cross section by about a factor of 10. This is shown in Figure 5. The scatter here is somewhat greater than for the mean cross sections, as might be expected. Once again it seems appropriate and highly desirable to broaden the data base through a concerted effort to reduce additional data already in the OPOS historical file or which builds in the ADCOM files.

#### CONSIDERATION OF LWIR CROSS SECTION

As indicated above, the AFAL has no significant LWIR data in hand.

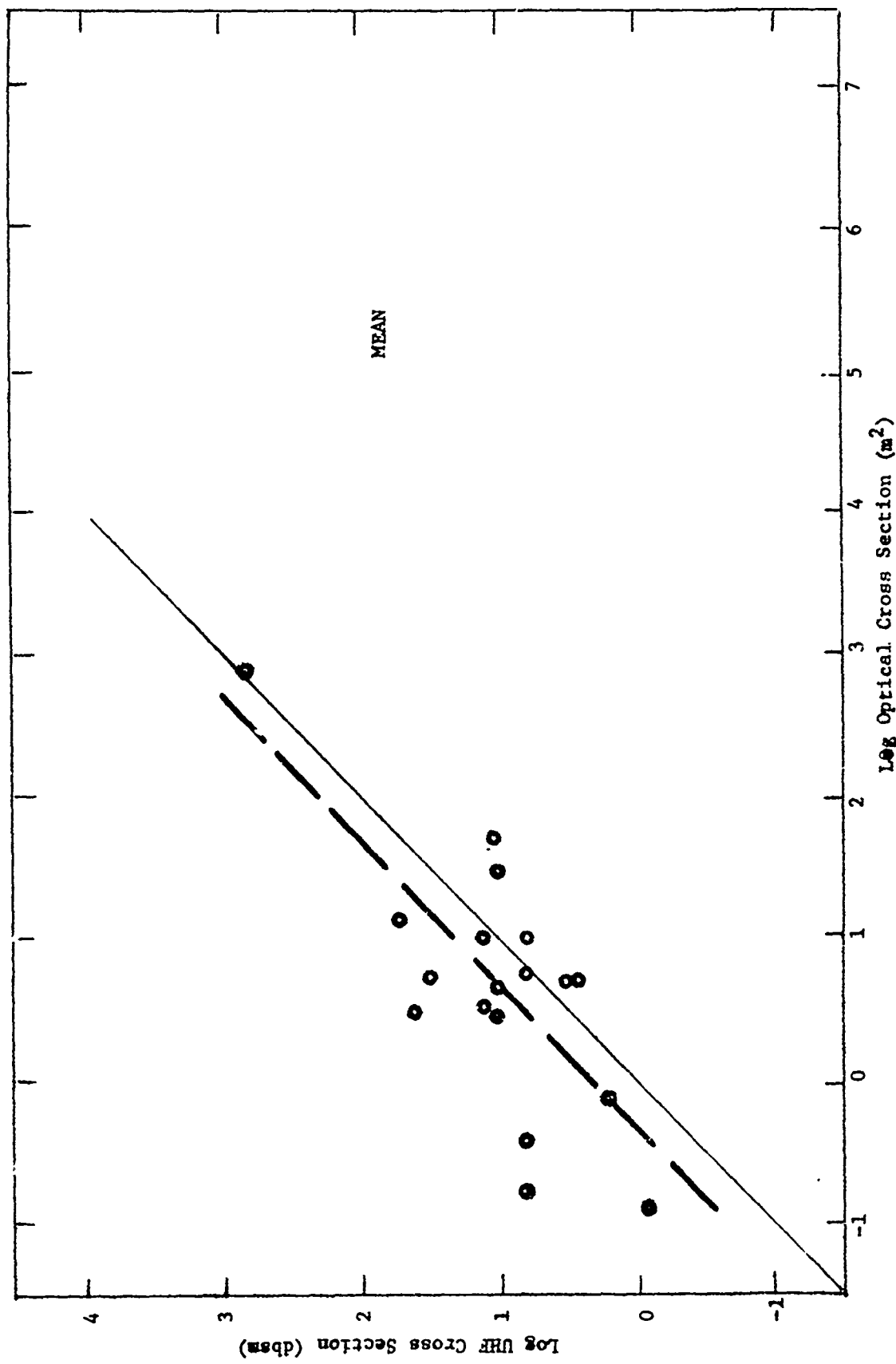


FIGURE 3. COMPARISON OF MEAN OPTICAL AND RADAR CROSS SECTIONS OF 18 SPACECRAFT FOR WHICH UHF DATA ARE AVAILABLE

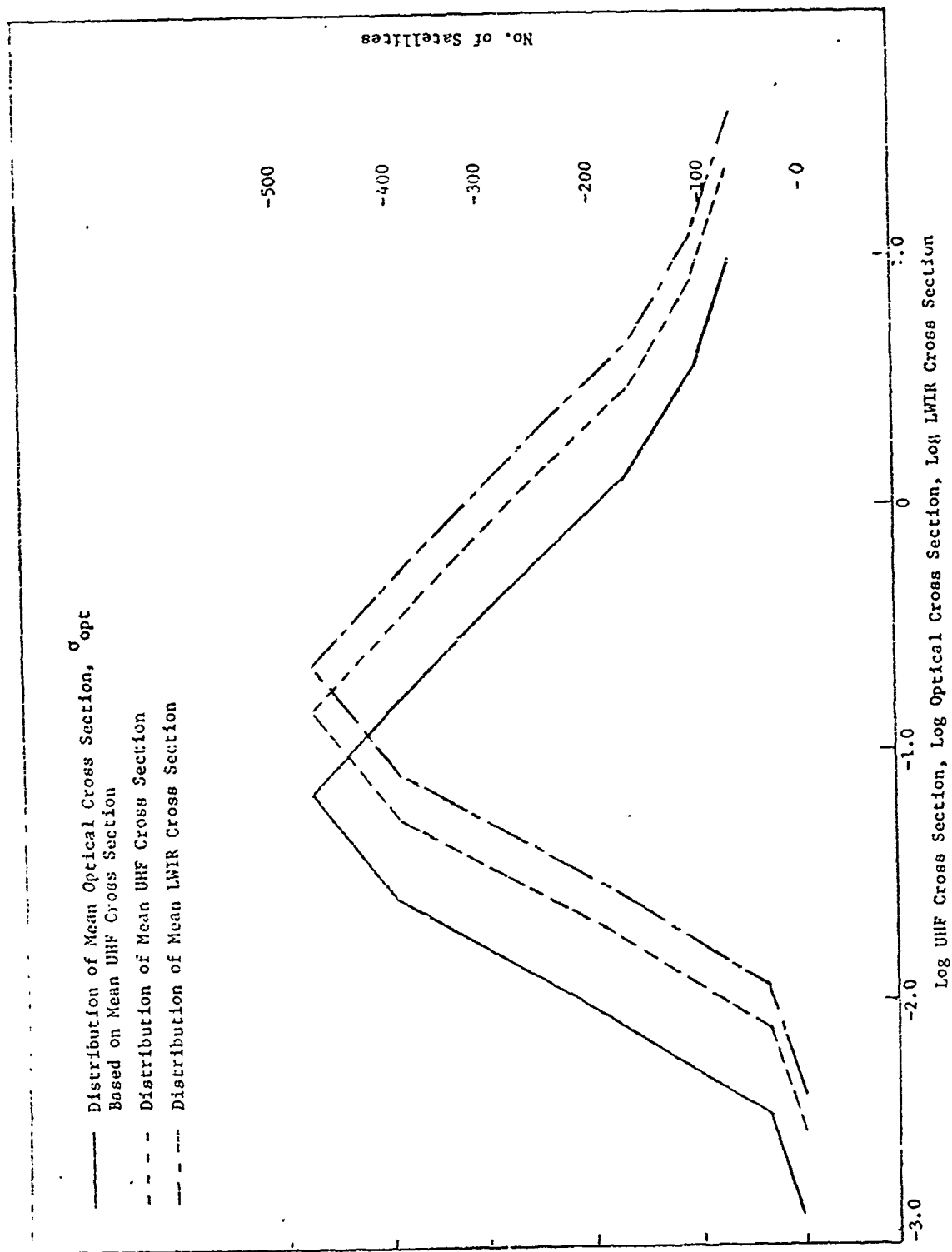


FIGURE 4. DERIVED CROSS SECTION POPULATIONS IN OPTICAL, LWIR, AND UHF REGIONS

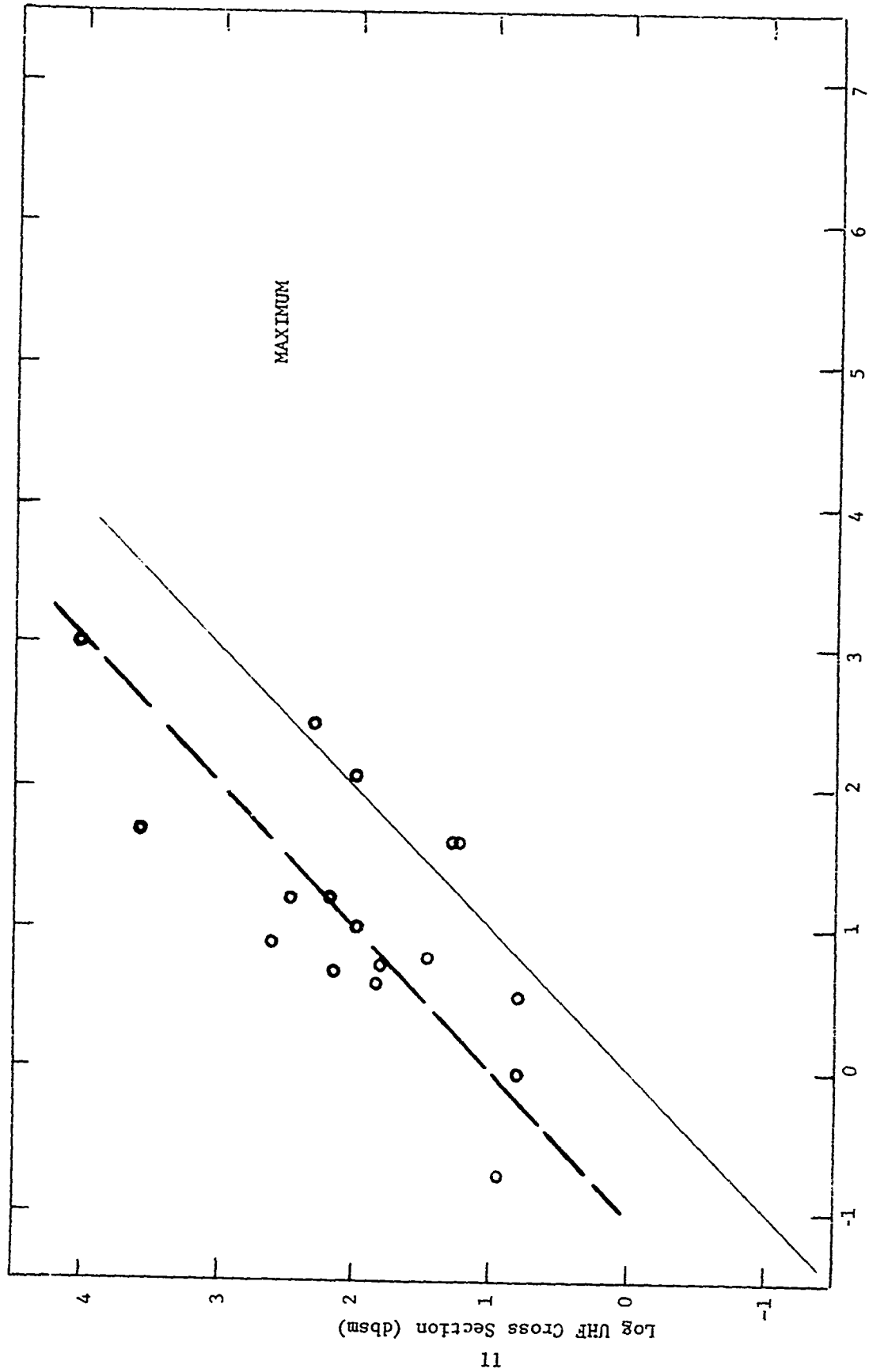


FIGURE 5. COMPARISON OF MAXIMUM OPTICAL AND RADAR CROSS SECTIONS OF 18 SPACECRAFT FOR WHICH UHF DATA ARE AVAILABLE

Some brief measurements were made in the late 1960's with a simple helium-cooled radiometer to show the feasibility of such measurements from a mountain-top observatory, and a follow-on multi-detector radiometer was installed at the AFAL Cloudcroft Observatory to use the 48-inch reflector as the collector, but few results were obtained before this effort was terminated. Separately we conducted some LWIR measurements of spacecraft from a B57-F aircraft using an LHe-chilled telescope of 8-inch aperture in 1970-71, but the quality and quantity of these data are not sufficient for the problem at hand. Here we will attempt to relate a scaling law to convert mean visual optical cross sections into mean LWIR cross sections. We believe it is important that data from other past and future programs be examined in the light of the relationships between LWIR cross section and radar and optical cross sections.

We will define the LWIR cross section as being the projected area of a perfectly emissive sphere of surface temperature  $300^{\circ}\text{K}$ . Thus a 44.4-inch perfectly black sphere at  $300^{\circ}\text{K}$  will have a 1-meter<sup>2</sup> LWIR cross section; at  $357^{\circ}\text{K}$  it will have a 2-meter<sup>2</sup> cross section; and at  $600^{\circ}\text{K}$  it will have a 16-meter<sup>2</sup> cross section in accordance with Stefan's law. The basis for this approximation can be found in Ref. 16.

In an appendix to this report, an approximation is developed which relates the LWIR cross section to the true geometric cross section and to the optical cross section. This approximation is good to no better than a factor of 4 and in special cases may be worse, but it does allow the use of the mean optical cross section population distribution to be further mapped into an approximation to a mean LWIR population distribution. This mean distribution is also shown in Figure 4. It must be used with suspicion since it rests on an empirical transformation of UHF to optical cross section and then an approximate transformation to the LWIR cross section. The wide range of solar absorptivities and LWIR emissivities which one can find on different surfaces of real spacecraft probably tends to make real objects merge toward "a mean" LWIR cross section, but it may not be the one adopted here. Because the LWIR cross section depends on the projected area seen by the observer and variations in the projected area are relatively small for practical space vehicles (only flat plate structures will change by more than a factor of 2 from the mean area to the maximum area), no attempt is made to consider a maximum LWIR cross section.

#### RECOMMENDATIONS

- (1) Efforts should be made in the near future to extend the data base of both mean and maximum optical cross section and a detailed study made of their relationship to the corresponding UHF cross section.
- (2) Some effort is warranted in validating the dependence of radar cross section with frequency on real space objects; this could be analytical or experimental, depending on the advice of radar experts. One data base might be comparisons of mean and maximum cross sections from Diyarbakir (L-band) and the other SPACETRACK sensors.
- (3) The key recommendation is that the unreduced or unpublished data be processed and published as soon as possible.

## APPENDIX

### Derivation of IR Scaling Relationship

The LWIR radiant intensity in a bandwidth from  $\lambda_1$  to  $\lambda_2$  from an object is:

$$J_{IR} = \frac{A\epsilon\sigma T^4 \Delta f}{\pi} \text{ watts/ster} \quad (1)$$

$A$  = Area (cross section) meter<sup>2</sup>  
 $\epsilon$  = Emissivity  
 $\sigma$  = Stefan-Boltzman constant ( $5.6686 \times 10^{-8} \text{ w/m}^2/\text{T}^4$ )  
 $T$  = Temperature ( $^{\circ}\text{K}$ )  
 $\Delta f$  =  $w_{\lambda_1-\lambda_2}/w_{0-\infty}$  ( $\text{w/m}^2/\text{w/m}^2$ ) (fraction in band)

In space, the surface temperature of a perfectly-insulated surface can be computed from the relationship:

$$\sigma T^4 = (H_s + H_a) \frac{\alpha}{\epsilon} + H_p \quad (2)$$

- $H_s$  = Average solar heat flux incident to surface  
 $H_a$  = Average albedo heat flux incident  
 $H_p$  = Average thermal earthshine heat flux incident  
 $\alpha$  = Solar absorptance

Although  $H_s$  can vary widely with orbital altitude and inclination and with surface-sun angle, a reasonable value taken from graphs appearing in the Handbook of Military Infrared Technology, 1965 (Ref. 17) is:

$$H_s = .85 S$$

$S$  = Solar constant  
= 1400 watts/m<sup>2</sup>

$H_a$  varies even more than  $H_s$  with altitude, time of year, cloud cover, ground conditions, sun-planet and planet-surface angles, etc. The average planet albedo as given in the IR Handbook is .36. From the curves for geometric factors in the Handbook, which account for orbital and surface angle conditions,

a value of .5 can be approximated for most conditions.  $H_a$  is then given by:

$$H_a = aS F_a$$

$$a = \text{albedo} = .36$$

$$F_a = \text{geometric factor} = .5$$

$H_0$  is the thermal earthshine. The IR Handbook approximates this value as that radiance emitted by a 250°K blackbody. Geometric factors are presented as for earth albedo and again a value of .5 will be used as in the albedo term. A spectral bandwidth of 8-14 $\mu$  will be used. Therefore:

$$H_0 = \sigma T^4 \Delta f F_0$$

And:

$$H_s = S .85 = 1400 \times .85 = 1190 \text{ watts/m}^2$$

$$H_a = aS F_a = .14 \times .36 \times .5 = 252 \text{ watts/m}^2$$

$$H_0 = (5.6686 \times 10^{-12}) (250)^4 (.32) (.5) \\ = 35.2 \text{ watts/m}^2$$

Thus in (2):

$$\sigma T^4 = (1190 + 252) \frac{\alpha}{\epsilon} + 35.2 \\ = (1442) \frac{\alpha}{\epsilon} + 35.2$$

From the IR Handbook, the lowest values of  $\frac{\alpha}{\epsilon}$ , chosen for thermal control, are approximately .2 and extend to greater than 5. So the lowest value of  $(H_s + H_a) \frac{\alpha}{\epsilon}$  is about 300 w/m<sup>2</sup>. The  $H_0$  term is .1 of this value, and for this approximation the  $H_0$  term will be neglected. Therefore:

$$\sigma T^4 \approx 1400 \frac{\alpha}{\epsilon}$$

Substituting in (1)

$$\begin{aligned} J_{\text{IR}} &= \frac{A\epsilon\Delta f}{\pi} \left(1400 \frac{\alpha}{\epsilon}\right) \\ &= \frac{A\Delta f\alpha}{\pi} \cdot 1400 \end{aligned}$$

For expected spacecraft temperatures and an 8-14 $\mu\text{m}$  bandwidth,  $\Delta f$  varies from about .3 to .4. An average value of .35 will be chosen

$$\begin{aligned} J_{\text{IR}} &= \frac{1400 \times .35}{\pi} A\alpha \\ &= 156 A\alpha \text{ watts/ster} \end{aligned}$$

In the above relationship we have used the physical projected cross section,  $A$ , which should be related to the visible cross section,  $A_v$ , only for the case of  $0^\circ$  phase angle (illumination from the direction of the observer) by the relationship

$$A_v = \rho A$$

where  $\rho$  is the reflectivity in visible region of the spectrum.

The relationship between the visible-region reflectivity and the solar absorptance is expressed as

$$\rho = 1 - \alpha$$

Thus we can write an approximate formal relationship between the IR radiant intensity as

$$J_{\text{IR}} = 156 \frac{\alpha}{1 - \alpha} A_v \quad (3)$$

We choose to use an LWIR standard of cross section as a sphere with an area-emissivity product of unity at a temperature of  $300^\circ\text{K}$ , that is

$$A\epsilon = 1 \text{ meter}^2$$

In the spectral band from 8 to 14 $\mu$ m, the reference 1 meter<sup>2</sup> target will have a radiant intensity of

$$J_o = \frac{A\epsilon\sigma (300)^4 \Delta f}{r}$$

$$= 51 \text{ EA w/ster}$$

Therefore, an object with  $J_{IR} = 102$  w/ster due either to a higher temperature or emissivity would have an IR cross section of

$$A_{IR} = \frac{J_{IR}}{J_o} = \frac{102}{51} = 2\text{m}^2$$

In general, we propose to deduce an approximate IR cross section from

$$A_{IR} = \frac{156 \alpha A_v}{J_o (1-\alpha)} = \frac{156 (\alpha)}{51 (1-\alpha)} A_v$$

$$A_{IR} = 3.1 \frac{(\alpha)}{(1-\alpha)} A_v \quad (4)$$

To use Equation (3) we must know or estimate the value of  $\alpha$ . Typical values for  $\alpha$  taken from the IR Handbook are shown in Table II.

TABLE II

<u>Material</u>	<u><math>\alpha</math></u>
Aluminum	
as received	.27-.41
cleaned	.18-.44
sand-blasted	~.6
foil	.17-.19
vacuum-deposited on mylar	.2
Glass on Silicon Solar Cell	.9
Gold Plate on Aluminum	.3
Graphite	.96
Inconel	.55-.89

Table II (contd)

<u>Material</u>	<u><math>\alpha</math></u>
White Paint	.2-.3
Black Paint	.89-.95
Si Solar Cell	.938
Stainless Steel	.4-.9

In examples below, it will be clear that choice of the correct value of  $\alpha$  is very important for the relationship (4) to give a reasonable approximation to the LWIR cross section. In addition, the emissivity  $\epsilon$  of the spacecraft surface is an important parameter controlling the LWIR cross section. Values of  $\epsilon$  range from 0.03 for highly reflective surfaces, such as the evaporated aluminum coating on PAGEOS, to 0.8 or 0.9 on specially blackened surfaces used as thermal radiators.

To develop a rationale for choice of a mean  $\alpha$ , consider three spherical objects, each  $1\text{m}^2$  projected area, but with surfaces representative of extremes in  $\alpha$  and  $\epsilon$ . ARPA 101 was a concept for an absorptive, emissive test satellite.

<u>ARPA 101</u>	<u>PAGEOS</u>	<u>White, Diffuse</u>
1	2	3
$A_1 = 1\text{m}^2$	$A_2 = 1\text{m}^2$	$A_3 = 1\text{m}^2$
$\alpha_1 = .8$	$\alpha_2 = .2$	$\alpha_3 = .2$
$\epsilon_1 = .8$	$\epsilon_2 = .05$	$\epsilon_3 = .8$

In the previous analysis, the surface temperature of an object could be calculated from the simplified expression:

$$\sigma T^4 = 1400 \frac{\alpha}{\epsilon}$$

$$\sigma T_1^4 = 1400 \text{ w/m}^2$$

$$\sigma T_2^4 = 5600 \text{ w/m}^2$$

$$\sigma T_3^4 = 350 \text{ w/m}^2$$

Now  $J = \frac{A \epsilon \sigma T^4}{\pi}$

$$J_1 = \frac{.8 (.35) 1400}{\pi} = 125 \text{ w/ster}$$

$$J_2 = \frac{.05 (.35) 5600}{\pi} = 31.2 \text{ w/ster}$$

$$J_3 = \frac{.8 (.35) 350}{\pi} = 31.2 \text{ w/ster}$$

Then the actual IR cross sections would be approximately

$$A'_1 = \frac{125}{51} = 2.45 \text{ m}^2$$

$$A'_2 = \frac{31.2}{51} = .612 \text{ m}^2$$

$$A'_3 = \frac{31.2}{51} = .612 \text{ m}^2$$

We would expect the observed optical cross sections to be given by

$$A_v = A (1-\alpha)$$

Then

$$A_{v1} = (1-.8) = .2 \text{ m}^2$$

$$A_{v2} = (1-.2) = .8 \text{ m}^2$$

$$A_{v3} = (1-.2) = .8 \text{ m}^2$$

If we assume a value for  $\alpha^2 = 0.53$

$$A_{IR} = 3.4 A_v$$

and we would predict an LWIR cross section sphere

Sphere	$A_{IR}$	$A'$	Factor
1	.676 m <sup>2</sup>	2.45 m <sup>2</sup>	3.6 low
2	2.7 m <sup>2</sup>	.612 m <sup>2</sup>	4.4 high
3	2.7 m <sup>2</sup>	.612 m <sup>2</sup>	4.4 high

While the accuracy of this estimation leaves much to be desired, the approximate relationship for estimating the LWIR cross section lies within a factor of 4 to 5.

It thus appears that the LWIR cross section will appear enhanced by a factor of 3 to 4 as a result of selective absorption and emission properties of common spacecraft surfaces.

To use the above approximate relationship, we use the mean UHF cross section with a shift in abscissa of  $0.53 - 0.34 = 0.19$  in the log or  $1.22 - 0.80 = 0.42$  in the ln (which the user should note was used in Ref 2, Figure C-2) so as to increase the cross section.

#### REFERENCES

1. Reference not listed intentionally.
2. W. E. Mabrey, H. F. Cash, and R. C. Rue, "A Method for Predicting and Generating Satellite Populations", DCS/Plans, Hq ADC, Ent AFB, Co (Dec 1971)
3. J. B. Zirker, F. L. Whipple, R. J. Davis, "Time Available for the Optical Observation of an Earth Satellite", Scientific Uses of Earth Satellites. University of Michigan Press, Ann Arbor, pp. 23-28. (1956)
4. K. E. Kissell, R. C. Vanderburgh, "Photoelectric Photometry - A Potential Source for Satellite Signatures." ARL TR 66-0162, (1966). Office of Aerospace Research, USAF.
5. R. C. Vanderburgh, "Photoelectric Measurements of Optical Glints from Orbiting Spacecraft", Proceedings of 1968 AFSC Science & Engineering Symposium, OAR 69-0003, (30 Oct-1 Nov 1968), pp J1-J28.
6. R. C. Vanderburgh, F. R. Vigneron, "Passive Optical Measurements of Alouette II Spin Dynamics", Space Research X, North Holland Publishing Co., Amsterdam, ARL TR 70-0253, pp. 37-42 (1970)
7. R. C. Vanderburgh, "Results of Field Testing and Inexpensive Transportable Photoelectric Satellite Tracking System", Space Research X, North Holland Publishing Co., Amsterdam, ARL TR 70-0256 (1970), pp. 17-20.
8. R. C. Vanderburgh, K. E. Kissell, "Measurements of Deformation and Spin Dynamics of the Pegasus Balloon-Satellite by Photoelectric Photometry". Planetary & Space Science, Vol. 19, pp. 223-231, (1971) ARL TR 71-0067. (April 1971)
9. R. C. Vanderburgh, K. E. Kissell, "Photoelectric Photometry of Quasi-Synchronous Spacecraft at the Cloudcroft Electro-Optical Site", ARL TR 71-0083.
10. Reference not listed intentionally.
11. R. C. Vanderburgh, "Photoelectric Photometry of Orbiting Spacecraft: Proven Data Collection and Interpretation Techniques", ARL MR 71-0006. (September 1971)
12. R. C. Vanderburgh, "Preliminary Report on the Results of Photoelectric Photometry of Space Objects Associated with the SESP 70-2 Launch of 7 August 1971", ARL MR 71-0007, (September 1971)

REFERENCES (cont.)

13. E. T. Tyson, R. C. Vanderburgh, K. E. Kissell, "Observational Data for the Satellite Observables Program", AFAL-TR-72-317, (November 1972)
14. R. C. Vanderburgh, K. E. Kissell, "Photometry of the United Kingdom Spacecraft Ariel-4, Space Object 5675, AFAL-TR-72-355, (May 1973)
15. K. E. Kissell, "Diagnosis of Spacecraft Surface Properties and Dynamical Motions by Optical Photometry", ARL 69-0082, (May 1969)
16. R. C. Vanderburgh, "Photoelectric Photometry of Orbiting Spacecraft: Proven Data Collection and Interpretation Techniques", ARL MR 71-0006, (September 1971)
17. Handbook of Military Infrared Technology (William L. Wolfe, Ed.), USGPO for ONR, Washington, D. C. (1965), pp. 804-811.